

Charged Particle Multiplicity in $e^+e^- \rightarrow q\bar{q}$ events at 161 and 172 GeV and from the Decay of the W Boson

DELPHI Collaboration

Abstract

The data collected by DELPHI in 1996 have been used to measure the average charged particle multiplicities and dispersions in $q\bar{q}$ events at centre-of-mass energies of $\sqrt{s} = 161$ GeV and $\sqrt{s} = 172$ GeV, and the average charge multiplicity in WW events at $\sqrt{s} = 172$ GeV. The multiplicities in $q\bar{q}$ events are consistent with the evolution predicted by QCD. The dispersions in the multiplicity distributions are consistent with Koba-Nielsen-Olesen (KNO) scaling. The average multiplicity of charged particles in hadronic W decays has been measured for the first time; its value, $19.23 \pm 0.74(stat + syst)$, is consistent with that expected for an e^+e^- interaction at a centre-of-mass energy equal to the W mass. The charged particle multiplicity in W decays shows no evidence of effects of colour reconnection between partons from different W's at the present level of statistics.

(To be submitted to Phys. Lett. B)

P.Abreu²¹, W.Adam⁴⁹, T.Adye³⁶, I.Ajinenko⁴¹, G.D.Alekseev¹⁶, R.Aleman⁴⁸, P.P.Allport²², S.Almehe²⁴, U.Amaldi⁹, S.Amato⁴⁶, P.Andersson⁴³, A.Andreazza⁹, P.Antilogus⁹, W-D.Apel¹⁷, Y.Arnoud¹⁴, B.Åsman⁴³, J-E.Augustin²⁵, A.Augustinus³⁰, P.Baillon⁹, P.Bambade¹⁹, F.Barao²¹, M.Barbi⁴⁶, D.Y.Bardin¹⁶, G.Barker⁹, A.Baroncelli³⁹, O.Barring²⁴, M.J.Bates³⁶, M.Battaglia¹⁵, M.Baubillier²³, J.Baudot³⁸, K-H.Becks⁵¹, M.Begalli⁶, P.Beilliere⁸, Yu.Belokopytov^{9,52}, K.Belous⁴¹, A.C.Benvenuti⁵, C.Berat¹⁴, M.Berggren⁴⁶, D.Bertini²⁵, D.Bertrand², M.Besancon³⁸, F.Bianchi⁴⁴, M.Bigi⁴⁴, M.S.Bilenky¹⁶, P.Billoir²³, M-A.Bizouard¹⁹, D.Bloch¹⁰, M.Blume⁵¹, M.Bonesini²⁷, W.Bonivento²⁷, M.Boonekamp³⁸, P.S.L.Booth²², A.W.Borgland⁴, G.Borisov^{38,41}, C.Bosio³⁹, O.Botner⁴⁷, E.Boudinov³⁰, B.Bouquet¹⁹, C.Bourdarios¹⁹, T.J.V.Bowcock²², M.Bozzo¹³, P.Branchini³⁹, K.D.Brand³⁵, T.Brenke⁵¹, R.A.Brenner⁴⁷, R.C.A.Brown⁹, P.Bruckman¹⁸, J-M.Brunet⁸, L.Bugge³², T.Buran³², T.Burgsmueller⁵¹, P.Buschmann⁵¹, S.Cabrera⁴⁸, M.Caccia²⁷, M.Calvi²⁷, A.J.Camacho Rozas⁴⁰, T.Camporesi⁹, V.Canale³⁷, M.Canepa¹³, F.Carena⁹, L.Carroll²², C.Caso¹³, M.V.Castillo Gimenez⁴⁸, A.Cattai⁹, F.R.Cavallo⁵, V.Chabaud⁹, Ph.Charpentier⁹, L.Chaussard²⁵, P.Checchia³⁵, G.A.Chelkov¹⁶, M.Chen², R.Chierici⁴⁴, P.Chliapnikov⁴¹, P.Chochula⁷, V.Chorowitz²⁵, J.Chudoba²⁹, V.Cindro⁴², P.Collins⁹, M.Colomer⁴⁸, R.Contri¹³, E.Cortina⁴⁸, G.Cosme¹⁹, F.Cossutti⁴⁵, J-H.Cowell²², H.B.Crawley¹, D.Crennell³⁶, G.Crosetti¹³, J.Cuevas Maestro³³, S.Czellar¹⁵, J.Dahm⁵¹, B.Dalmagne¹⁹, G.Damgaard²⁸, P.D.Dauncey³⁶, M.Davenport⁹, W.Da Silva²³, A.Deghorain², G.Della Ricca⁴⁵, P.Delpierre²⁶, N.Demaria³⁴, A.De Angelis⁹, W.De Boer¹⁷, S.De Brabandere², C.De Clercq², C.De La Vaissiere²³, B.De Lotto⁴⁵, A.De Min³⁵, L.De Paula⁴⁶, H.Dijkstra⁹, L.Di Ciaccio³⁷, A.Di Diodato³⁷, A.Djannati⁸, J.Dolbeau⁸, K.Doroba⁵⁰, M.Dracos¹⁰, J.Drees⁵¹, K.-A.Drees⁵¹, M.Dris³¹, J-D.Durand^{25,9}, D.Edsall¹, R.Ehret¹⁷, G.Eigen⁴, T.Ekelof⁴⁷, G.Ekspong⁴³, M.Elsing⁹, J-P.Engel¹⁰, B.Erzen⁴², M.Espirito Santo²¹, E.Falk²⁴, G.Fanourakis¹¹, D.Fassouliotis⁴⁵, M.Feindt⁹, A.Fenyuk⁴¹, P.Ferrari²⁷, A.Ferrer⁴⁸, S.Fichet²³, T.A.Filippas³¹, A.Firestone¹, P.-A.Fischer¹⁰, H.Foeth⁹, E.Fokitis³¹, F.Fontanelli¹³, F.Formenti⁹, B.Franek³⁶, A.G.Frodesen⁴, R.Fruhworth⁴⁹, F.Fulda-Quenzer¹⁹, J.Fuster⁴⁸, A.Galloni²², D.Gamba⁴⁴, M.Gandelman⁴⁶, C.Garcia⁴⁸, J.Garcia⁴⁰, C.Gaspar⁹, U.Gasparini³⁵, Ph.Gavillet⁹, E.N.Gaziz³¹, D.Gele¹⁰, J-P.Gerber¹⁰, L.Gerdyukov⁴¹, R.Gokheli⁵⁰, B.Golob⁴², P.Goncalves²¹, G.Gopal³⁶, L.Gorn¹, M.Gorski⁵⁰, Yu.Gouz^{44,52}, V.Gracco¹³, E.Graziani³⁹, C.Green²², A.Grefrath⁵¹, P.Gris³⁸, G.Grosdidier¹⁹, K.Grzelak⁵⁰, M.Gunther⁴⁷, J.Guy³⁶, F.Hahn⁹, S.Hahn⁵¹, Z.Hajduk¹⁸, A.Hallgren⁴⁷, K.Hamacher⁵¹, F.J.Harris³⁴, V.Hedberg²⁴, R.Henriques²¹, J.J.Hernandez⁴⁸, P.Herquet², H.Herr⁹, T.L.Hessing³⁴, J.-M.Heuser⁵¹, E.Higon⁴⁸, S-O.Holmgren⁴³, P.J.Holt³⁴, D.Holthuizen³⁰, S.Hoorelbeke², M.Houlden²², J.Hrubic⁴⁹, K.Huet², K.Hultqvist⁴³, J.N.Jackson²², R.Jacobsson⁴³, P.Jalocha⁹, R.Janik⁷, Ch.Jarlskog²⁴, G.Jarlskog²⁴, P.Jarry³⁸, B.Jean-Marie¹⁹, E.K.Johansson⁴³, L.Jonsson²⁴, P.Jonsson²⁴, C.Joram⁹, P.Juillot¹⁰, M.Kaiser¹⁷, F.Kapusta²³, K.Karafasoulis¹¹, E.Karvelas¹¹, S.Katsanevas²⁵, E.C.Katsoufis³¹, R.Keranen⁴, Yu.Khokhlov⁴¹, B.A.Khomenko¹⁶, N.N.Khovanski¹⁶, B.King²², N.J.Kjaer³⁰, O.Klapp⁵¹, H.Klein⁹, P.Kluit³⁰, D.Knoblach¹⁷, P.Kokkinias¹¹, M.Koratzinos⁹, K.Korcyl¹⁸, V.Kostioukhine⁴¹, C.Kourkoumelis³, O.Kouznetsov¹⁶, M.Krammer⁴⁹, C.Kreuter⁹, I.Kronkvist²⁴, J.Krstic¹¹, Z.Krumstein¹⁶, W.Krupinski¹⁸, P.Kubinec⁷, W.Kucewicz¹⁸, K.Kurvinen¹⁵, C.Lacasta⁹, I.Laktineh²⁵, J.W.Lamsa¹, L.Lanceri⁴⁵, D.W.Lane¹, P.Langefeld⁵¹, J-P.Laugier³⁸, R.Lauhakangas¹⁵, G.Leder⁴⁹, F.Ledroit¹⁴, V.Lefebvre², C.K.Legan¹, A.Leisos¹¹, R.Leitner²⁹, J.Lemonne², G.Lenzen⁵¹, V.Lepeltier¹⁹, T.Lesiak¹⁸, M.Lethuillier³⁸, J.Libby³⁴, D.Liko⁹, A.Lipniacka⁴³, I.Lippi³⁵, B.Loerstad²⁴, J.G.Loken³⁴, J.M.Lopez⁴⁰, D.Loukas¹¹, P.Lutz³⁸, L.Lyons³⁴, J.MacNaughton⁴⁹, G.Maehlum¹⁷, J.R.Mahon⁶, A.Maio²¹, T.G.M.Malmgren⁴³, V.Malychev¹⁶, F.Mandl⁴⁹, J.Marco⁴⁰, R.Marco⁴⁰, B.Marechal⁴⁶, M.Margoni³⁵, J-C.Marin⁹, C.Mariotti⁹, A.Markou¹¹, C.Martinez-Rivero³³, F.Martinez-Vidal⁴⁸, S.Marti i Garcia²², J.Masik²⁹, F.Matorras⁴⁰, C.Matteuzzi²⁷, G.Matthiae³⁷, M.Mazzucato³⁵, M.Mc Cubbin²², R.Mc Kay¹, R.Mc Nulty⁹, G.Mc Pherson²², J.Medbo⁴⁷, C.Meroni²⁷, S.Meyer¹⁷, W.T.Meyer¹, M.Michelotto³⁵, E.Migliore⁴⁴, L.Mirabito²⁵, W.A.Mitaroff⁴⁹, U.Mjoernmark²⁴, T.Moa⁴³, R.Moeller²⁸, K.Moenig⁹, M.R.Monge¹³, P.Moretini¹³, H.Mueller¹⁷, K.Muenich⁵¹, M.Mulders³⁰, L.M.Mundim⁶, W.J.Murray³⁶, B.Muryn^{14,18}, G.Myatt³⁴, T.Myklebust³², F.Naraghi¹⁴, F.L.Navarria⁵, S.Navas⁴⁸, K.Nawrocki⁵⁰, P.Negri²⁷, S.Nemecek¹², W.Neumann⁵¹, N.Neumeister⁴⁹, R.Nicolaidou³, B.S.Nielsen²⁸, M.Nieuwenhuizen³⁰, V.Nikolaenko^{10,16}, P.Niss⁴³, A.Nomerotski³⁵, A.Normand²², A.Nygren²⁴, W.Oberschulte-Beckmann¹⁷, V.Obraztsov⁴¹, A.G.Olshevski¹⁶, A.Onofre²¹, R.Orava¹⁵, G.Orazi¹⁰, S.Ortuno⁴⁸, K.Osterberg¹⁵, A.Ouraou³⁸, P.Paganini¹⁹, M.Paganoni^{9,27}, S.Paiano⁵, R.Pain²³, H.Palka¹⁸, Th.D.Papadopoulou³¹, K.Papageorgiou¹¹, L.Pape⁹, C.Parkes³⁴, F.Parodi¹³, U.Parzefall²², A.Passeri³⁹, M.Pegoraro³⁵, L.Peralta²¹, H.Pernegger⁴⁹, M.Pernicka⁴⁹, A.Perrotta⁵, C.Petridou⁴⁵, A.Petrolini¹³, H.T.Phillips³⁶, G.Piana¹³, F.Pierre³⁸, M.Pimenta²¹, E.Piotto³⁵, T.Podobnik³⁴, O.Podobrin⁹, M.E.Pol⁶, G.Polak¹⁸, P.Poropat⁴⁵, V.Pozdniakov¹⁶, P.Privitera³⁷, N.Pukhaeva¹⁶, A.Pullia²⁷, D.Radojicic³⁴, S.Ragazzi²⁷, H.Rahmani³¹, P.N.Ratoff²⁰, A.L.Read³², M.Reale⁵¹, P.Rebecchi⁹, N.G.Redaeli²⁷, M.Regler⁴⁹, D.Reid⁹, R.Reinhardt⁵¹, P.B.Renton³⁴, L.K.Resvanis³, F.Richard¹⁹, J.Ridky¹², G.Rinaudo⁴⁴, O.Rohne³², A.Romero⁴⁴, P.Ronchese³⁵, L.Roos²³, E.I.Rosenberg¹⁵, P.Rosinsky⁷, P.Roudeau¹⁹, T.Rovelli⁵, V.Ruhmann-Kleider³⁸, A.Ruiz⁴⁰, K.Rybicki¹⁸, H.Saarikou¹⁵, Y.Sacquin³⁸, A.Sadovsky¹⁶, G.Sajot¹⁴, J.Salt⁴⁸, M.Sannino¹³, H.Schneider¹⁷, U.Schwickerath¹⁷, M.A.E.Schyns⁵¹, G.Sciolla⁴⁴, F.Scuri⁴⁵, P.Seager²⁰, Y.Sedykh¹⁶, A.M.Segar³⁴, A.Seitz¹⁷, R.Sekulin³⁶, L.Serbelloni³⁷, R.C.Shellard⁶, A.Sheridan²², P.Siegrist^{9,38}, R.Silvestre³⁸, F.Simonetto³⁵, A.N.Sisakian¹⁶, T.B.Skaali³², G.Smadja²⁵, N.Smirnov⁴¹, O.Smirnova²⁴, G.R.Smith³⁶, O.Solovianov⁴¹, R.Sosnowski⁵⁰, D.Souza-Santos⁶, T.Spassov²¹, E.Spiriti³⁹, P.Sponholz⁵¹, S.Squarcia¹³, D.Stamper⁹, C.Stanescu³⁹, S.Stanic⁴², S.Stapnes³², I.Stavitski³⁵, K.Stevenson³⁴, A.Stocchi¹⁹, J.Strauss⁴⁹, R.Strub¹⁰, B.Stugu⁴, M.Szczekowski⁵⁰, M.Szeptycka⁵⁰, T.Tabarelli²⁷, J.P.Tavernet²³

O.Tchikilev⁴¹, F.Tegenfeldt⁴⁷, F.Terranova²⁷, J.Thomas³⁴, A.Tilquin²⁶, J.Timmermans³⁰, L.G.Tkatchev¹⁶, T.Todorov¹⁰, S.Todorova¹⁰, D.Z.Toet³⁰, A.Tomaradze², B.Tome²¹, A.Tonazzo²⁷, L.Tortora³⁹, G.Transtromer²⁴, D.Treille⁹, G.Tristram⁸, A.Trombini¹⁹, C.Troncon²⁷, A.Tsirou⁹, M-L.Turluer³⁸, I.A.Tyapkin¹⁶, M.Tyndel³⁶, S.Tzamarias¹¹, B.Ueberschaer⁵¹, O.Ullaland⁹, V.Uvarov⁴¹, G.Valenti⁵, E.Vallazza⁴⁵, G.W.Van Apeldoorn³⁰, P.Van Dam³⁰, J.Van Eldik³⁰, A.Van Lysebette², N.Vassilopoulos³⁴, G.Vegni²⁷, L.Ventura³⁵, W.Venus³⁶, F.Verbeure², M.Verlato³⁵, L.S.Vertogradov¹⁶, D.Vilanova³⁸, P.Vincent²⁵, L.Vitale⁴⁵, E.Vlasov⁴¹, A.S.Vodopyanov¹⁶, V.Vrba¹², H.Wahlen⁵¹, C.Walck⁴³, F.Waldner⁴⁵, C.Weiser¹⁷, A.M.Wetherell⁹, D.Wicke⁵¹, J.H.Wickens², M.Wielers¹⁷, G.R.Wilkinson⁹, W.S.C.Williams³⁴, M.Winter¹⁰, M.Witek¹⁸, T.Wlodek¹⁹, J.Yi¹, K.Yip³⁴, O.Yushchenko⁴¹, F.Zach²⁵, A.Zaitsev⁴¹, A.Zalewska⁹, P.Zalewski⁵⁰, D.Zavrtanik⁴², E.Zevgolatakos¹¹, N.I.Zimin¹⁶, G.C.Zucchelli⁴³, G.Zumerle³⁵

¹Department of Physics and Astronomy, Iowa State University, Ames IA 50011-3160, USA

²Physics Department, Univ. Instelling Antwerpen, Universiteitsplein 1, B-2610 Wilrijk, Belgium and IHEP, ULB-VUB, Pleinlaan 2, B-1050 Brussels, Belgium

and Faculté des Sciences, Univ. de l'Etat Mons, Av. Maistriau 19, B-7000 Mons, Belgium

³Physics Laboratory, University of Athens, Solonos Str. 104, GR-10680 Athens, Greece

⁴Department of Physics, University of Bergen, Allégaten 55, N-5007 Bergen, Norway

⁵Dipartimento di Fisica, Università di Bologna and INFN, Via Irnerio 46, I-40126 Bologna, Italy

⁶Centro Brasileiro de Pesquisas Físicas, rua Xavier Sigaud 150, RJ-22290 Rio de Janeiro, Brazil

and Depto. de Física, Pont. Univ. Católica, C.P. 38071 RJ-22453 Rio de Janeiro, Brazil

and Inst. de Física, Univ. Estadual do Rio de Janeiro, rua São Francisco Xavier 524, Rio de Janeiro, Brazil

⁷Comenius University, Faculty of Mathematics and Physics, Mlynska Dolina, SK-84215 Bratislava, Slovakia

⁸Collège de France, Lab. de Physique Corpusculaire, IN2P3-CNRS, F-75231 Paris Cedex 05, France

⁹CERN, CH-1211 Geneva 23, Switzerland

¹⁰Institut de Recherches Subatomiques, IN2P3 - CNRS/ULP - BP20, F-67037 Strasbourg Cedex, France

¹¹Institute of Nuclear Physics, N.C.S.R. Demokritos, P.O. Box 60228, GR-15310 Athens, Greece

¹²FZU, Inst. of Physics of the C.A.S. High Energy Physics Division, Na Slovance 2, 180 40, Praha 8, Czech Republic

¹³Dipartimento di Fisica, Università di Genova and INFN, Via Dodecaneso 33, I-16146 Genova, Italy

¹⁴Institut des Sciences Nucléaires, IN2P3-CNRS, Université de Grenoble 1, F-38026 Grenoble Cedex, France

¹⁵Helsinki Institute of Physics, HIP, P.O. Box 9, FIN-00014 Helsinki, Finland

¹⁶Joint Institute for Nuclear Research, Dubna, Head Post Office, P.O. Box 79, 101 000 Moscow, Russian Federation

¹⁷Institut für Experimentelle Kernphysik, Universität Karlsruhe, Postfach 6980, D-76128 Karlsruhe, Germany

¹⁸Institute of Nuclear Physics and University of Mining and Metallurgy, Ul. Kawiora 26a, PL-30055 Krakow, Poland

¹⁹Université de Paris-Sud, Lab. de l'Accélérateur Linéaire, IN2P3-CNRS, Bât. 200, F-91405 Orsay Cedex, France

²⁰School of Physics and Chemistry, University of Lancaster, Lancaster LA1 4YB, UK

²¹LIP, IST, FCUL - Av. Elias Garcia, 14-1^o, P-1000 Lisboa Codex, Portugal

²²Department of Physics, University of Liverpool, P.O. Box 147, Liverpool L69 3BX, UK

²³LPNHE, IN2P3-CNRS, Universités Paris VI et VII, Tour 33 (RdC), 4 place Jussieu, F-75252 Paris Cedex 05, France

²⁴Department of Physics, University of Lund, Sölvegatan 14, S-22363 Lund, Sweden

²⁵Université Claude Bernard de Lyon, IPNL, IN2P3-CNRS, F-69622 Villeurbanne Cedex, France

²⁶Univ. d'Aix - Marseille II - CPP, IN2P3-CNRS, F-13288 Marseille Cedex 09, France

²⁷Dipartimento di Fisica, Università di Milano and INFN, Via Celoria 16, I-20133 Milan, Italy

²⁸Niels Bohr Institute, Blegdamsvej 17, DK-2100 Copenhagen 0, Denmark

²⁹NC, Nuclear Centre of MFF, Charles University, Areal MFF, V Holesovickach 2, 180 00, Praha 8, Czech Republic

³⁰NIKHEF, Postbus 41882, NL-1009 DB Amsterdam, The Netherlands

³¹National Technical University, Physics Department, Zografou Campus, GR-15773 Athens, Greece

³²Physics Department, University of Oslo, Blindern, N-1000 Oslo 3, Norway

³³Dpto. Física, Univ. Oviedo, Avda. Calvo Sotelo, S/N-33007 Oviedo, Spain, (CICYT-AEN96-1681)

³⁴Department of Physics, University of Oxford, Keble Road, Oxford OX1 3RH, UK

³⁵Dipartimento di Fisica, Università di Padova and INFN, Via Marzolo 8, I-35131 Padua, Italy

³⁶Rutherford Appleton Laboratory, Chilton, Didcot OX11 0QX, UK

³⁷Dipartimento di Fisica, Università di Roma II and INFN, Tor Vergata, I-00173 Rome, Italy

³⁸CEA, DAPNIA/Service de Physique des Particules, CE-Saclay, F-91191 Gif-sur-Yvette Cedex, France

³⁹Istituto Superiore di Sanità, Ist. Naz. di Fisica Nucl. (INFN), Viale Regina Elena 299, I-00161 Rome, Italy

⁴⁰Instituto de Física de Cantabria (CSIC-UC), Avda. los Castros, S/N-39006 Santander, Spain, (CICYT-AEN96-1681)

⁴¹Inst. for High Energy Physics, Serpukov P.O. Box 35, Protvino, (Moscow Region), Russian Federation

⁴²J. Stefan Institute, Jamova 39, SI-1000 Ljubljana, Slovenia and Department of Astroparticle Physics, School of

Environmental Sciences, Kostanjevska 16a, Nova Gorica, SI-5000 Slovenia,

and Department of Physics, University of Ljubljana, SI-1000 Ljubljana, Slovenia

⁴³Fysikum, Stockholm University, Box 6730, S-113 85 Stockholm, Sweden

⁴⁴Dipartimento di Fisica Sperimentale, Università di Torino and INFN, Via P. Giuria 1, I-10125 Turin, Italy

⁴⁵Dipartimento di Fisica, Università di Trieste and INFN, Via A. Valerio 2, I-34127 Trieste, Italy

and Istituto di Fisica, Università di Udine, I-33100 Udine, Italy

⁴⁶Univ. Federal do Rio de Janeiro, C.P. 68528 Cidade Univ., Ilha do Fundão BR-21945-970 Rio de Janeiro, Brazil

⁴⁷Department of Radiation Sciences, University of Uppsala, P.O. Box 535, S-751 21 Uppsala, Sweden

⁴⁸IFIC, Valencia-CSIC, and D.F.A.M.N., U. de Valencia, Avda. Dr. Moliner 50, E-46100 Burjassot (Valencia), Spain

⁴⁹Institut für Hochenergiephysik, Österr. Akad. d. Wissensch., Nikolsdorfergasse 18, A-1050 Vienna, Austria

⁵⁰Inst. Nuclear Studies and University of Warsaw, Ul. Hoza 69, PL-00681 Warsaw, Poland

⁵¹Fachbereich Physik, University of Wuppertal, Postfach 100 127, D-42097 Wuppertal, Germany

⁵²On leave of absence from IHEP Serpukhov

1 Introduction

The average charged particle multiplicity is one of the basic observables characterizing hadronic final states. It has been extensively studied both theoretically and experimentally, and results for $e^+e^- \rightarrow q\bar{q}$ events exist at several centre-of-mass energies [1].

The data collected at LEP in 1996 are at the highest available centre-of-mass energies in e^+e^- interactions, 161 and 172 GeV, and a new physics window is opened: the production and decay of W boson pairs. The cross-section for WW production rises rapidly from about 3 pb at 161 GeV to about 12 pb at 172 GeV. Besides the study of the evolution of charged multiplicity with energy, this channel is important because it allows a comparison of the average charged multiplicity in W hadronic decays when both Ws decay in fully hadronic modes with the case in which one of the Ws decays semileptonically. These two multiplicities should be equal in the absence of interference between the products of the hadronic decay of the Ws.

The possible presence of interference (due to colour reconnection and Bose-Einstein correlations [2–6]) in hadronic decays of WW pairs has been discussed on a theoretical basis, in the framework of the measurement of the W mass. A first measurement of Bose-Einstein correlations in WW events has shown, within the limited statistics, no evidence for such correlations between pions from different Ws [7]. A qualitative argument shows that the effect of colour reconnection between the decay products of different Ws could affect the charged multiplicity: the presence of two cross-talking dijets in the fully hadronic WW decay allows the evolving particle system to pick states with smaller invariant mass than in the case of independent dijets with no cross-talk. In a recently proposed model [4], this correlation could lead to a charged multiplicity for a WW system in which both Ws decay hadronically that is significantly smaller than twice the multiplicity of a W whose partner decays semileptonically. In addition, effects of colour reconnection are expected to be considerably enhanced in kinematic regions where there is strong overlap between jets originating from different Ws. On the other hand, Bose-Einstein correlations are predicted to increase the multiplicity in WW events in some models [6].

In this paper, the data recorded using the DELPHI detector [8,9] have been used to determine the average and the dispersion of the charge multiplicity distributions in $q\bar{q}$ events at 161 and 172 GeV and in WW events at 172 GeV. The multiplicity in $q\bar{q}$ events is compared with the evolution predicted by QCD. The multiplicity in W decays is discussed as a probe for correlations between the W decay products. Since no significant difference is found between the fully hadronic and the mixed hadronic-leptonic decay modes, both are used to extract the first determination of the average charged multiplicity in W decays.

The paper is structured as follows. Section 2 describes the detector, the data sample and the track selection. Section 3 describes the selection and analysis of $q\bar{q}$ data. Section 4 describes the selection and analysis of WW data. Finally, in Section 5, results are discussed and conclusions are drawn.

2 Data Sample and Event preselection

During 1996, DELPHI collected data at centre-of-mass energies around 161 GeV and around 172 GeV with integrated luminosities of 9.96 pb^{-1} and of 10.14 pb^{-1} respectively.

A preselection of hadronic events in both samples was made, requiring at least 6 charged particles with momentum p above $400 \text{ MeV}/c$, angle θ with respect to the beam direction between 20° and 160° , a track length of at least 30 cm in the Time Projection

Chamber (DELPHI's main tracking detector), a distance of closest approach to the interaction point less than 4 cm in the plane perpendicular to the beam axis and less than 10 cm along the beam axis, and a total energy of the charged particles above 0.15 times the centre-of-mass energy \sqrt{s} . In the calculation of the energies E , all charged particles were assumed to have the pion mass.

Charged particles were then used in the analysis if they had $p > 100$ MeV/ c , a relative error on the momentum measurement $\Delta p/p < 1$, polar angle $20^\circ < \theta < 160^\circ$, a track length of at least 30 cm in the TPC, and a distance of closest approach to the primary vertex smaller than 3 cm in the plane perpendicular to the beam axis and 6 cm along the beam axis.

The influence of the detector on the analysis was studied with the full DELPHI simulation program, DELSIM [9]. Events were generated with PYTHIA 5.7 and JETSET 7.4 [10], with parameters tuned to fit LEP1 data from DELPHI [11]. The Parton Shower (PS) model was used. The particles were followed through the detailed geometry of DELPHI giving simulated digitizations in each detector. These data were processed with the same reconstruction and analysis programs as the real data. The sizes of the simulated samples were 20995 $q\bar{q}\gamma$ and 4806 WW events at 161 GeV; 62823 $q\bar{q}\gamma$ and 27546 WW events at 172 GeV. In addition, 100,000 events without Initial State Radiation effects were generated with JETSET/PYTHIA for each energy and channel, in order to compute the average charged multiplicity and dispersion at generator level. In the WW case two samples were generated, one with two W bosons and the other with only one W with energy equal to half the centre-of-mass energy; for both samples only hadronic W decays were generated.

To check the ability of the simulation to model the efficiency for the reconstruction of charged particles, the sample of 0.9 pb^{-1} collected at the Z during 1996 was used. From this sample, by integrating the distribution of $\xi_E = -\ln(2E/\sqrt{s})$ corrected bin by bin using the simulation, the average charged particle multiplicity at the Z was measured to be $20.98 \pm 0.04(stat)$, in good agreement with the world average of 20.99 ± 0.14 [12]. A "multiplicity scale" uncertainty of 0.7% can thus be assumed in addition to the systematic errors quoted below.

3 Analysis of $q\bar{q}$ decays

3.1 Charged multiplicity in $q\bar{q}$ events at 161 GeV

The cross-section for $e^+e^- \rightarrow q\bar{q}(\gamma)$ above the Z peak is dominated by radiative $q\bar{q}\gamma$ events; the initial state radiated photons (ISR photons) are generally aligned along the beam direction and not detected. In order to compute the hadronic centre-of-mass energy, the procedure described in [13] was used. The procedure clusters the particles into two jets using the Durham algorithm [14], excluding candidate ISR photons. Assuming an ISR photon along the beam pipe if no candidate ISR photon has been detected, the energy of the ISR photon is computed from the jet directions assuming massless kinematics. The effective centre-of-mass energy of the hadronic system, $\sqrt{s'}$, is calculated as the invariant mass of the system recoiling from the ISR photon. The spectrum of the calculated energies for the events collected at 161 GeV is shown in Figure 1. The full width at half maximum of the peak corresponding to the radiative return to the Z is about 10 GeV, in agreement with simulation. The small contribution from WW pairs is shown in the same figure.

The method used to obtain the hadronic centre-of-mass energy overestimates the true energy in the case of double hard radiation in the initial state. For instance, if the

two ISR photons are emitted back to back, the remaining two jets may also be back to back, but with energy much smaller than the beam energy. Cutting on the total energy measured in the detector reduces the contamination from such events. Events with reconstructed hadronic centre-of-mass energy ($\sqrt{s'}$) above 150 GeV, with total energy seen in the detector above 105 GeV, and with at least 9 charged particles with momentum above 100 MeV/c, were used to compute the multiplicity at 161 GeV. A total of 282 events were selected.

The background from WW events was estimated from the simulation to be 7.9 events. The contamination from double radiative returns to the Z (within 10 GeV of the nominal Z mass) was estimated from the simulation to be around 2%. The analysis procedure described below corrects for this effect.

The measured average multiplicity of charged particles with $p > 0.1$ GeV/c, after subtraction of the WW background events, was $22.54 \pm 0.40(stat)$, to be compared to $22.75 \pm 0.12(stat)$ in the $q\bar{q}$ PS simulation including detector effects. The dispersion of the multiplicity distribution in the data was $6.55 \pm 0.28(stat)$, to be compared to $6.63 \pm 0.08(stat)$ in the $q\bar{q}$ PS simulation. After correcting for detector effects, the average charged multiplicity was found to be $\langle n_{ch} \rangle = 25.45 \pm 0.45(stat)$, and the dispersion to be $D = 7.80 \pm 0.34(stat)$. These values include the products of the decays of particles with lifetime $\tau < 10^{-9}$ s, in particular K_S^0 and Λ .

The average multiplicity was also computed by integrating the distributions of rapidity $y = \frac{1}{2} \ln \frac{E-p_{\parallel}}{E+p_{\parallel}}$ with respect to the thrust axis, and of $\xi_E = -\ln(2E/\sqrt{s})$, both distributions having been corrected bin by bin using the simulation. In the calculation of the energies, all particles were again assumed to have the pion mass. The ξ_E distribution was integrated up to a value of 6.2, and the extrapolation to the region above this cut was based on the simulation at generator level.

For the central value for the measurement of the charged multiplicity, the result of the integration of the ξ_E distribution was taken, since the detection efficiency depends mostly on the momentum of the particle. The maximum shift of this value with respect to the values from the other methods, 0.28, was included in the systematic error. The systematic errors due to the statistics of the Monte Carlo samples were found to be 0.1, both for the multiplicity (with ξ_E) and for the dispersion, and were added in quadrature to the systematic errors.

Half of the value from the extrapolation in ξ_E , 0.04, was also added in quadrature to the systematic error. The average charged multiplicity in the selected events, including the above corrections, was 25.19 and 25.46 from the y and ξ_E distributions respectively, consistent with the value, 25.45, obtained from the average observed multiplicity. In the selected events, one is integrating over hadronic energies above 150 GeV. By comparing the multiplicity and the dispersion obtained using JETSET PS at 161 GeV with the average values above 150 GeV from the energy spectrum of the selected events in the simulation, the values of $\langle n_{ch} \rangle$ and D were found to differ by 0.21 and 0.10 respectively. The analysis procedure corrects for these differences and they were also added in quadrature to the systematic error.

Finally, for the centre-of-mass energy of 161 GeV, the values

$$\langle n_{ch} \rangle = 25.46 \pm 0.45(stat) \pm 0.37(syst) \quad (1)$$

$$D = 7.80 \pm 0.34(stat) \pm 0.14(syst) \quad (2)$$

were obtained for the average charged multiplicity and for the dispersion. The systematic errors were obtained by adding in quadrature the contributions from the sources above.

3.2 Charged multiplicity in $q\bar{q}$ events at 172 GeV

Events with reconstructed hadronic centre-of-mass energy ($\sqrt{s'}$) above 155 GeV were used to compute the multiplicity at 172 GeV.

A total of 235 hadronic events were selected by requiring that the multiplicity for charged particles (with $p > 100$ MeV/ c) was larger than 9, that the total energy of the charged particles exceeded $0.2\sqrt{s}$, and that the narrow jet broadening [15] was smaller than 0.1. The distribution of the narrow jet broadening for the data, compared to the expectations from simulation, is shown in Figure 2. From the simulation it was calculated that the expected background coming from WW events was 4.1 ± 0.1 events. The contamination from double radiative returns to the Z (within 10 GeV of the nominal Z mass) was estimated by simulation to be around 3%.

The average multiplicity of charged particles with $p > 0.1$ GeV/ c measured in the selected events, after subtraction of the WW background estimated by simulation, was $22.25 \pm 0.44(stat)$, to be compared to $22.04 \pm 0.06(stat)$ in the $q\bar{q}$ PS simulation including detector effects. The dispersion of the multiplicity distribution in the data was $6.69 \pm 0.31(stat)$, to be compared to the dispersion from the $q\bar{q}$ PS simulation of $6.39 \pm 0.04(stat)$. After correcting for detector effects, the average charged multiplicity was found to be $\langle n_{ch} \rangle = 26.60 \pm 0.53(stat)$, and the dispersion to be $D = 8.46 \pm 0.40(stat)$. These values again include the products of the decays of particles with lifetime $\tau < 10^{-9}$ s.

The average multiplicity was also computed, as in Section 3.1, by integrating the distributions of rapidity with respect to the thrust axis and of ξ_E . The ξ_E distribution was integrated up to a value of 6.2, and the extrapolation to the region above this cut was based on the simulation at generator level. Half of the value from that extrapolation, 0.07, was added in quadrature to the systematic error. The average charged multiplicity of the selected events, including the above corrections, is 26.78 and 26.52 respectively from the y and ξ_E distribution, consistent with the value from the average observed multiplicity.

To estimate the systematic error associated with the procedure to remove the contribution from the WW events, the value of the cut on the narrow jet broadening was varied from 0.06 to 0.14 in steps of 0.02. The new values for the average charged multiplicity and the dispersion were stable within these variations, and the highest shifts with respect to the previous results, 0.38 and 0.45 respectively, were added in quadrature to the systematic error. The effect of the uncertainty on the WW cross-section was found to be negligible.

By comparing the multiplicity and the dispersion obtained using JETSET PS at 172 GeV with the average value above 155 GeV from the energy spectrum of the selected events, it was found that the values of $\langle n_{ch} \rangle$ and D differ by 0.27 and 0.13 respectively. These shifts were added in quadrature to the systematic error. As a central value for the measurement of the charged multiplicity the result of the integration of the ξ_E distribution was taken, since the detection efficiency depends mostly on the momentum of the particle. The maximum shift with respect to the values obtained with the previous methods, 0.26, was added in quadrature to the systematic error. The systematic errors due to the statistics of the Monte Carlo samples were found to be 0.06, both for the multiplicity (with ξ_E) and for the dispersion, and were added in quadrature to the systematic errors.

Finally, for the centre-of-mass energy of 172 GeV, the values

$$\langle n_{ch} \rangle = 26.52 \pm 0.53(stat) \pm 0.54(syst) \quad (3)$$

$$D = 8.46 \pm 0.40(stat) \pm 0.47(syst) \quad (4)$$

were obtained for the average charged multiplicity and for the dispersion. The systematic errors were obtained by adding in quadrature the contributions from the sources above.

4 Analysis of WW decays

The analysis of WW decays was performed only on the 172 GeV data, since the sample collected at that energy was significantly larger than that at 161 GeV.

4.1 Fully hadronic channel ($WW \rightarrow 4j$)

Events with both Ws decaying into $q\bar{q}$ are characterized by high multiplicity, large visible energy, and tendency of the particles to be grouped in 4 jets. The events were pre-selected by requiring at least 12 charged particles (with $p > 400$ MeV/c), with a total energy (charged plus neutral) above 20% of the centre-of-mass energy.

The background at 172 GeV is dominated by $q\bar{q}(\gamma)$ events. For these events, the hadronic centre-of-mass energy was computed as described in the previous section. To remove the radiative hadronic events, the hadronic centre-of-mass energy was required to be above 110 GeV.

The particles in the event were forced to 4 jets using the Durham algorithm, and the events were kept if all jets had charged multiplicity larger than 1. It was also required that the separation between the jets (y_{cut} value) be larger than 0.005. The combination of these two cuts removed most of the remaining semi-leptonic WW decays and the 2-jet and 3-jet events of the $q\bar{q}$ background.

A four constraint fit was applied, imposing energy and momentum conservation except along the beam line, and the equality of the two dijet masses. Of the three fits obtained by permutation of the jets, the one with the best χ^2 was selected. Events were accepted only if the product of the smallest fitted jet energy and the smallest angle between the fitted jet directions was greater than 13 GeV·rad.

The purity and the efficiency of the selected data sample were estimated using simulation to be about 68% and 73% respectively. The data sample consists of 58 events, where 57 are expected from simulation. The expected background was subtracted bin by bin from the observed distributions. The values of $\langle n_{ch} \rangle$ before and after the background subtraction were 34.5 and 35.4 respectively.

The final value of $\langle n_{ch} \rangle$ was estimated by integrating the ξ_E distribution. To account for inefficiencies due to detector effects and selection criteria, a correction factor was computed, bin by bin, as the ratio of the ξ_E distributions at generator level and after full simulation of the DELPHI detector and application of the above cuts. The following final value was obtained:

$$\langle N_{had}^{(HAD)}(2W) \rangle = 40.6 \pm 1.7(stat) \pm 1.1(syst), \quad (5)$$

where the systematic error accounts for variation of the selection criteria (0.8), change of the $q\bar{q}$ cross-sections within the error of the measured value [16] (0.04), uncertainty on the modelling of the background (0.64), and limited statistics in the simulated sample (0.08). The value of $\langle n_{ch} \rangle$ was also estimated from the observed multiplicity distribution as $40.3 \pm 1.7(stat)$, and the difference (0.36) from the reference value was taken as an extra systematic error. The uncertainty on the modelling of the background quoted above is the sum in quadrature of three contributions:

- Uncertainty on the multiplicity at 172 GeV. A relative uncertainty as in Eq. (3) was assumed; this gives a multiplicity error of 0.43.

- Uncertainty on the modelling of the 4-jet rate. The agreement between data and simulation was studied in a sample of 4-jet events at the Z, with y_{cut} ranging from 0.003 to 0.005. The rate of 4-jet events in the simulated sample was found to reproduce the data within 10%. The correction due to background subtraction was correspondingly varied by 10%, which gives an uncertainty of 0.16.
- Uncertainty on the multiplicity in 4-jet events. The average multiplicity of 4-jet events selected at the Z for a value of $y_{cut} = 0.005$ is larger by $(2.8 \pm 1.3(stat))\%$ than the corresponding value in the simulation. A shift by 2.8% in the multiplicity for 4-jet events induces a shift of 0.45 on the value in Eq. (5).

The presence of interference between the jets coming from the different Ws could create subtle effects, such as to make the application of the fit imposing equal masses inadequate. For this reason a different four constraint fit was performed, leaving the dijet masses free and imposing energy-momentum conservation. Of the three possible combinations of the four jets into WW pairs, the one with minimum mass difference was selected. No χ^2 cut was imposed in this case. The average multiplicity obtained was 41.4, again fully consistent with (5).

4.2 Mixed Hadronic and Leptonic Final States ($WW \rightarrow 2j\ell\nu$)

Events in which one W decays into lepton plus neutrino and the other one into quarks are characterized by two hadronic jets, one energetic isolated charged lepton, and missing momentum resulting from the neutrino. The main backgrounds to these events are radiative $q\bar{q}$ production and four-fermion final states containing two quarks and two oppositely charged leptons of the same flavour.

Events were selected by requiring seven or more charged particles, with a total energy (charged plus neutral) above $0.2\sqrt{s}$. Events in the $q\bar{q}\gamma$ final state with ISR photons at small polar angles, which would be lost inside the beam pipe, were suppressed by requiring the polar angle of the missing momentum vector to satisfy $|\cos \theta_{miss}| < 0.94$.

Including the missing momentum as an additional massless neutral particle (the candidate neutrino), the particles in the event were forced to 4 jets using the Durham algorithm. The jet for which the fractional jet energy carried by the highest momentum charged particle was greatest was considered as the “lepton jet”. The most energetic charged particle in the lepton jet was considered the lepton candidate, and the event was rejected if its momentum was smaller than 10 GeV/c or greater than 65 GeV/c. The “neutrino jet” was considered the jet clustered around the missing momentum. The event was discarded if the invariant mass of the 2 hadronic jets was smaller than 20 GeV/c².

At this point three alternative topologies were considered:

- Muon sample: when the lepton candidate was tagged as a muon and its isolation angle, with respect to other charged particles above 1 GeV/c, was above 10°, the event was accepted either if the lepton momentum was greater than 20 GeV/c, or if it was greater than 10 GeV/c and the value of the y_{cut} parameter required by the Durham algorithm to force the event from a 3-jet to a 4-jet configuration was greater than 0.003.
- Electron sample: when the lepton candidate had associated electromagnetic energy deposited in the calorimeters larger than 20 GeV, and isolation angle (defined as above) greater than 10 degrees, the event was accepted if the required value of y_{cut} was greater than 0.003.
- Inclusive sample: the events were also accepted if the “lepton” momentum was larger than 20 GeV/c and greater than half of the jet energy, the missing momentum was

larger than $0.1\sqrt{s}$, the required value of y_{cut} was greater than 0.003, and no other charged particle above 1 GeV/ c existed in the lepton jet.

All three topologies were then retained for the analysis, giving 33 events in the data sample. The estimated purity was 90%, and the efficiency was 54% (64% in the electron channel, 81% in the muon channel and 17% in the τ channel). A total of 30 events were expected from simulation. A correction was estimated from simulation to account for detector effects and the contribution from the initial lepton (or its decay products) to the observed multiplicity, taking as reference the sample generated with one W decaying into hadrons. The values of the observed charged multiplicity before and after the background subtraction were 16.9 and 16.8 respectively.

Finally the following value was obtained for the charged multiplicity for one W decaying hadronically in a WW event with mixed hadronic and leptonic final states by integrating the ξ_E distribution:

$$\langle N_{had}^{(SL)}(W) \rangle = 18.0 \pm 0.9(stat) \pm 0.6(syst), \quad (6)$$

where the systematic error accounts for the variation of the selection criteria (0.42), variation of the $q\bar{q}(\gamma)$ cross-sections within the error of the measured value [16] (negligible), limited statistics in the simulated samples (0.06) and the difference between the estimates of the charged multiplicity obtained from the ξ_E integration and from the alternative method of taking the average of the observed multiplicity distribution (0.43).

5 Discussion

Figure 3 shows the value of the average charged particle multiplicity in $e^+e^- \rightarrow q\bar{q}$ events at 161 GeV and 172 GeV compared with lower energy points from TASSO [17], HRS [18], and AMY [19], with DELPHI results in $q\bar{q}\gamma$ events at the Z [20], with the world average at the Z [12], with the LEP results at 133 GeV [13,21–23], and with L3 and OPAL values at 161–172 GeV [24,25]. A point corresponding to the multiplicity observed by DELPHI in W decays is also included at $\sqrt{s} = M_W$ and is discussed later in this section. The value at the Z has been lowered by 0.20, to account for the different proportion of $b\bar{b}$ and $c\bar{c}$ events at the Z with respect to the continuum $e^+e^- \rightarrow q\bar{q}$ [26]. Similarly, the values at 133, 161 and 172 GeV were lowered by 0.15, 0.12 and 0.11 respectively.

The QCD prediction for charged multiplicity has been computed as a function of α_s including the resummation of leading (LLA) and next-to-leading (NLLA) corrections [27,13]:

$$n_{ch}(\sqrt{s}) = a[\alpha_s(\sqrt{s})]^b e^{c/\sqrt{\alpha_s(\sqrt{s})}} \left[1 + d \cdot \sqrt{\alpha_s(\sqrt{s})} \right],$$

where s is the squared centre-of-mass energy and a is a parameter (not calculable from perturbation theory) whose value has been fitted from the data. The constants $b = 0.49$ and $c = 2.27$ are predicted by the theory [27] and $\alpha_s(\sqrt{s})$ is the strong coupling constant. The parameter d was introduced [20] to allow for higher order corrections. A fit to data between 20 GeV and $\sqrt{s} = M_Z$, with $\alpha_s(\sqrt{s})$ (expressed at next-to-leading order) and a and d as free parameters, is shown in Figure 3. The results of the fit are: $a = 0.053 \pm 0.006$, $d = 1.11 \pm 0.39$, and $\alpha_s(m_Z) = 0.119 \pm 0.003(stat)$. This value of $\alpha_s(m_Z)$ yields $\alpha_s(172 \text{ GeV}) = 0.108 \pm 0.002(stat)$, and the curve describes the data well.

The ratios of the average multiplicity to the dispersion, $\langle n_{ch} \rangle / D$, measured at 161 GeV and 172 GeV, are consistent with the average from the measurements at lower centre-of-mass energies (3.12 ± 0.05), as can be seen in Figure 4. This is consistent with

KNO scaling [28], and also with the predictions of QCD including 1-loop Higher Order terms (H.O.) [29].

From the results obtained on hadronic W decays, we observe that the charged multiplicity from WW systems in which both Ws decay hadronically is consistent with twice that from a W whose partner decays semileptonically:

$$\frac{2 \langle N_{had}^{(SL)}(W) \rangle}{\langle N_{had}^{(had)}(2W) \rangle} = 0.89 \pm 0.06(stat) \pm 0.04(syst). \quad (7)$$

The ratio above is three standard deviations smaller than the ratio (1.11) obtained by applying our selection efficiency to the prediction in [4] in case of complete colour reconnection, folded around 90 degrees because quarks were not distinguished from antiquarks in this analysis.

A possible dependence of the charged multiplicity in WW fully hadronic events on the minimum angle between two jets, suggested in [4], was checked by dividing the sample into two sub-samples according to the smallest interjet angle θ_j in the event, (a) $\theta_j < 60^\circ$ and (b) $\theta_j > 60^\circ$. The distribution of the angle θ_j for data and simulation is shown in Figure 5. The average multiplicities measured (including corrections for detector effects) were consistent: $42.9 \pm 2.5(stat)$ in sample (a) and $38.6 \pm 2.3(stat)$ in sample (b). The ratio r of the average multiplicities in sample (b) to sample (a) is

$$r = 0.90 \pm 0.07(stat) \pm 0.03(syst) \quad (8)$$

where the systematic error accounts for the different background correction in the two regions (the result was $0.95 \pm 0.06(stat)$ before background subtraction). The ratio obtained by applying the prediction in [4] to the observed θ_j distribution is 1.08, which is larger than the measurement by 2.3 standard deviations.

Thus, at the present level of statistics, the study of charged multiplicity in W decays shows no evidence of colour reconnection effects.

In the hypothesis (consistent with this analysis) that the charged multiplicity in a W decay is independent of the decay mode of the other W, the measurements can be averaged to obtain the best determination of the charged particle multiplicity from hadronic decays of the W. Considering the systematic errors as independent:

$$\langle N(W) \rangle = 19.23 \pm 0.74(stat + syst), \quad (9)$$

where the error is the sum in quadrature of the statistical and of the systematic contributions. The value of $N(W)$ is also plotted in Figure 3 at an energy value corresponding to the W mass; it has been increased by 0.35 units to account for the different proportion of events with a b or a c quark in WW decays than in continuum e^+e^- events [26]. It lies on the same curve as the e^+e^- data.

Acknowledgements

We are greatly indebted to our technical collaborators and to the funding agencies for their support in building and operating the DELPHI detector. Very special thanks are due to the members of the CERN-SL Division for the excellent performance of the LEP collider. Thanks to Jorge Dias de Deus, to Alberto Giovannini and to Valery Khoze for comments on the manuscript.

References

- [1] For a review see for example G.D. Lafferty et al., J. Phys. **G21** (1995) A1.
- [2] T. Sjöstrand and V.A. Khoze, Z. Phys. **C62** (1994) 281.
- [3] B.R. Webber, in “QCD Event Generators”, in “Physics at LEP2”, eds. G. Altarelli, T. Sjöstrand and F. Zwirner, CERN 96-01 Vol 2, (1996) 161.
- [4] J. Ellis and K. Geiger, “Signatures of Parton Exogamy in $e^+e^- \rightarrow W^+W^- \rightarrow hadrons$ ”, CERN-TH/97-46.
- [5] L. Lönnblad and T. Sjöstrand, Phys. Lett. **B351** (1995) 293.
- [6] V. Kartvelishvili, R. Kvatadze and R. Moeller, “Estimating the effects of Bose-Einstein correlations on the W mass measurement at LEP 2”, Manchester Preprint MC-TH-97/04.
- [7] DELPHI Coll., P. Abreu et al., Phys. Lett. **B401** (1997) 181.
- [8] DELPHI Coll., P. Abreu et al., Nucl. Instr. Meth. **A303** (1991) 233.
- [9] DELPHI Coll., P. Abreu et al., Nucl. Instr. Meth. **A378** (1996) 57.
- [10] T. Sjöstrand, Comp. Phys. Comm. **82** (1994) 74.
- [11] DELPHI Coll., P. Abreu et al., Z. Phys. **C77** (1996) 11.
- [12] R.M. Barnett et al. (Particle Data Group), Phys. Rev. **D54** (1996) 1.
- [13] DELPHI Coll., P. Abreu et al., Phys. Lett. **B372** (1996) 172.
- [14] S. Bethke et al., Nucl. Phys. **B370** (1992) 310.
- [15] Yu.L. Dokshitzer, Phys. Lett. **B305** (1993) 295;
P. Nason and B.R. Webber, , in “QCD”, in “Physics at LEP2”, eds. G. Altarelli, T. Sjöstrand and F. Zwirner, CERN 96-01 Vol 1, (1996) 256.
- [16] A. Behrmann et al., “Delphi results on the measurement of fermion pair production for Z peak and higher energies at LEP for the winter 1997 Conferences”, DELPHI Note 97-31 PHYS 684.
- [17] TASSO Coll., W. Braunschweig et al., Z. Phys. **C45** (1989) 193.
- [18] HRS Coll., M. Derrick et al., Phys. Rev. **D34** (1987) 3304.
- [19] AMY Coll., H. Zheng et al., Phys. Rev. **D42** (1990) 737.
- [20] DELPHI Coll., P. Abreu et al., Z. Phys. **C70** (1996) 179.
- [21] ALEPH Coll., D. Buskulic et al., Z. Phys. **C73** (1997) 409.
- [22] L3 Coll., M. Acciarri et al., Phys. Lett. **B371** (1996) 137.
- [23] OPAL Coll., G. Alexander et al., Z. Phys. **C72** (1996) 191.
- [24] L3 Coll., “QCD Studies and Determination of α_s in e^+e^- collisions at $\sqrt{s} = 161$ GeV and 172 GeV”, CERN-PPE/97-42, submitted to Phys. Lett. **B**.
- [25] OPAL Coll., K. Ackerstaff et al., “QCD Studies with e^+e^- Annihilation Data at 161 GeV”, CERN-PPE/97-15, submitted to Z. Phys. **C**.
- [26] A. De Angelis, “Light Quark Hadrons in Hadronic Z Decays”, CERN-PPE/95-135, in Proc. EPS-HEP Conference, Bruxelles 1995, p.63.
- [27] B.R. Webber, Phys. Lett. **B143** (1984) 501 and references therein.
- [28] Z. Koba et al., Nucl. Phys. **B40** (1972) 317.
- [29] B. R. Webber, “QCD Cascade Approach to Jet Fragmentation”, in *Proc. XV Int. Symp. on Multiparticle Dynamics*, Lund 1984, Eds. G. Gustafson and C. Peterson (World Scientific, Singapore, 1984).

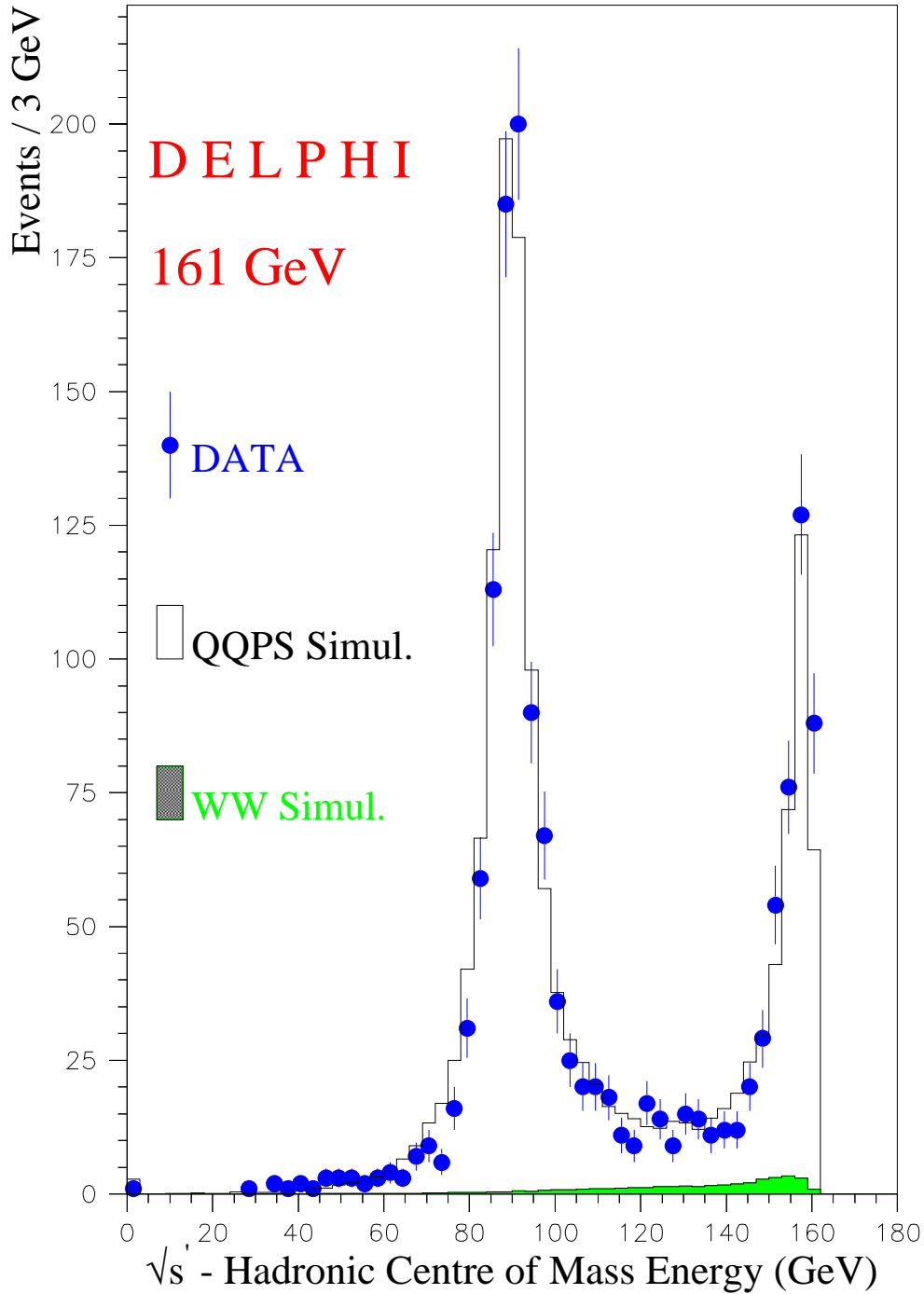


Figure 1: Distribution of the reconstructed hadronic centre-of-mass energy in $e^+e^- \rightarrow q\bar{q}$ events at 161 GeV for data (points) and for simulation (solid line). The simulation is the sum of two contributions: the white area represents the $q\bar{q}$ contribution simulated with PYTHIA Parton Shower model (QQPS in the label) and the hatched area represents the contribution from WW events. Data and simulation are normalized to the same number of events.

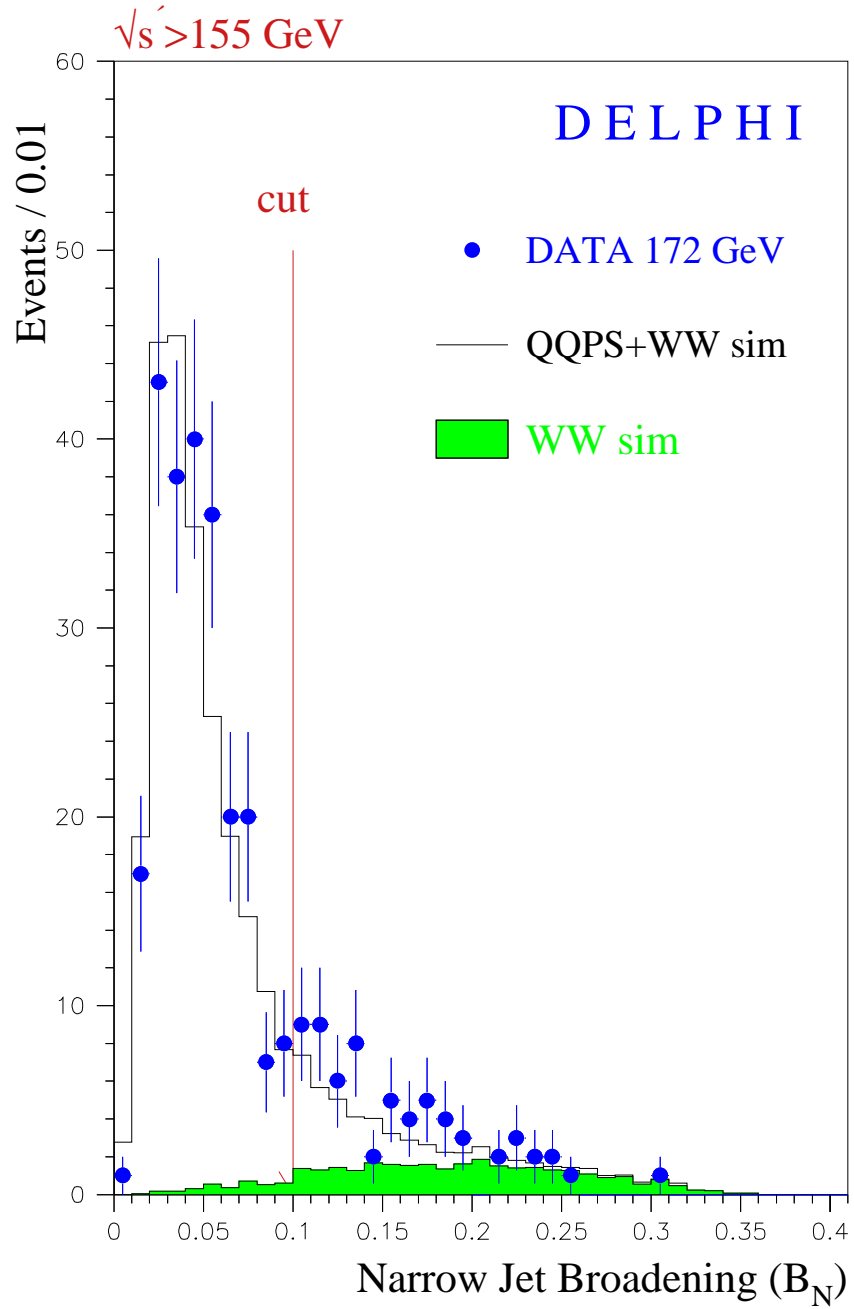


Figure 2: Narrow Jet Broadening distribution, as defined in [15], for the selected data events compared with that expected from simulation.

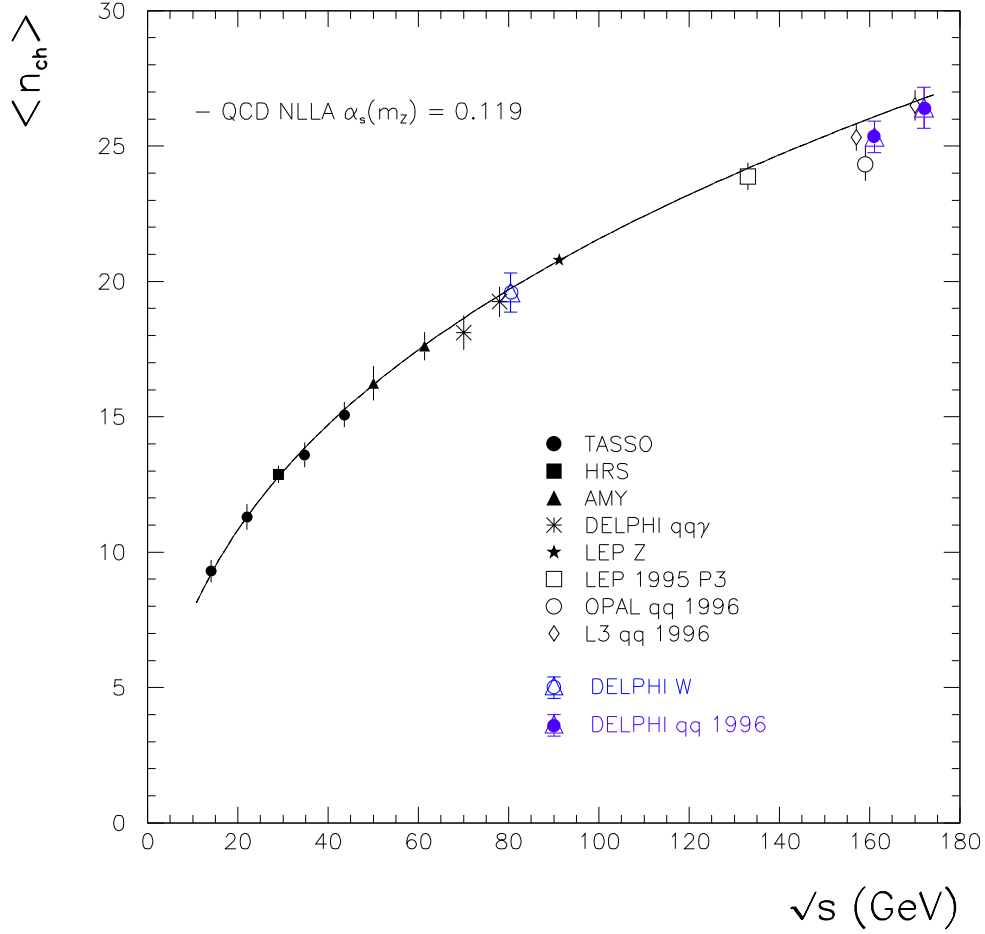


Figure 3: Measured average charged multiplicity in $e^+e^- \rightarrow q\bar{q}$ events as a function of centre-of-mass energy \sqrt{s} . DELPHI high energy results are compared with other experimental results and with a fit to a prediction from QCD in Next to Leading Order. The average charged multiplicity in W decays is also shown at an energy corresponding to the W mass. The measurements have been corrected for the different proportions of $b\bar{b}$ and $c\bar{c}$ events at the various energies.

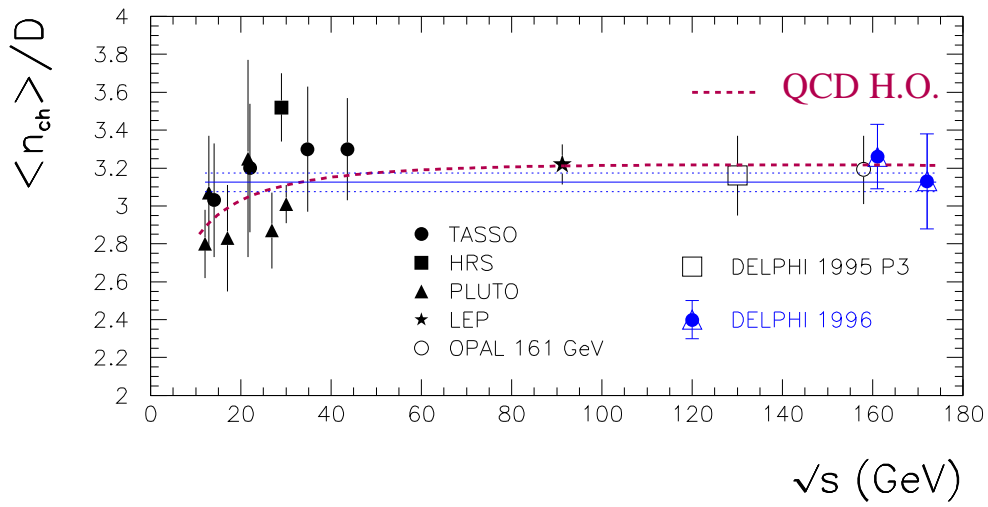


Figure 4: Ratio of the average charged multiplicity to the dispersion in $e^+e^- \rightarrow q\bar{q}$ events at 161 GeV and 172 GeV, compared with lower energy measurements. The straight solid and dotted lines represent the weighted average of the data points and its error. The dashed line represents the prediction from QCD (see text).

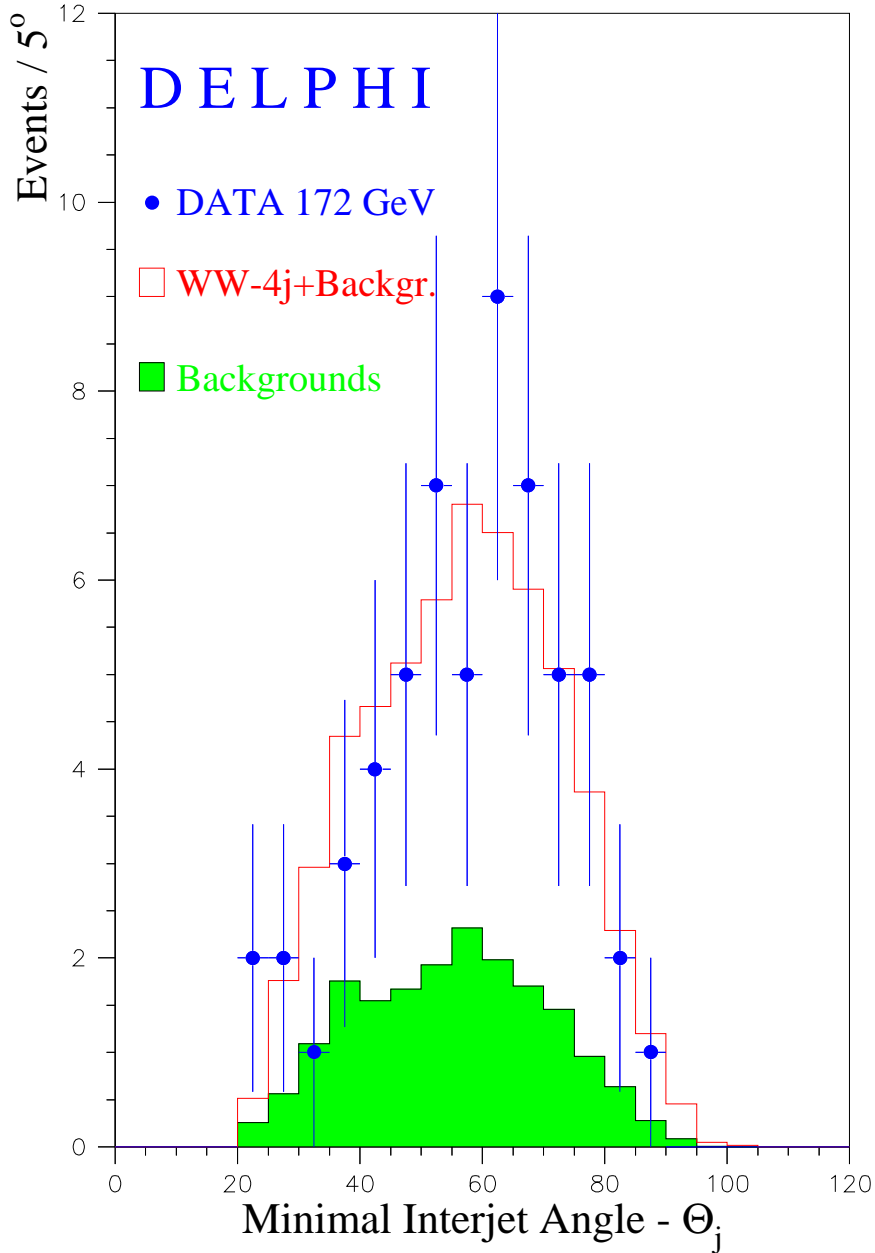


Figure 5: Distribution of θ_j , the smallest angle between any two fitted jet directions in $e^+e^- \rightarrow WW$ candidates, for events in which both Ws decay hadronically. The data (points) are compared with the simulation. The shaded area shows the simulated background.